International Journal of Mechanical, Industrial and Aerospace Sciences
ISSN: 2517-9950
Vol:9, No:12, 2015

Effect of Reynolds Number on Flow past a Square Cylinder in Presence of Upstream and Downstream Flat Plate at Small Gap Spacing

Shams-ul-Islam, Raheela Manzoor, Zhou Chao Ying

***Abstract*—**A two-dimensional numerical study for flow past a square cylinder in presence of flat plate both at upstream and downstream position is carried out using the single-relaxation-time lattice Boltzmann method for gap spacing 0.5 and 1. We select Reynolds numbers from 80 to 200. The wake structure mechanism within gap spacing and near wake region, vortex structures around and behind the main square cylinder in presence of flat plate are studied and compared with flow pattern around a single square cylinder. The results are obtained in form of vorticity contour, streamlines, power spectra analysis, time trace analysis of drag and lift coefficients. Four different types of flow patterns were observed in both configurations, named as (i) Quasi steady flow (QSF), (ii) steady flow (SF), (iii) shear layer reattachment (SLR), (iv) single bluff body (SBB). It is observed that upstream flat plate plays a vital role in significant drag reduction. On the other hand, rate of suppression of vortex shedding is high for downstream flat plate case at low Reynolds numbers. The reduction in mean drag force and root mean square value of drag force for upstream flat plate case are89.1% and 86.3% at (Re, g) = (80, 0.5d) and (120, 1d) and reduction for downstream flat plate case for mean drag force and root mean square value of drag force are 11.10% and 97.6% obtained at (180, 1d) and (180, 0.5d).

***Keywords*—**Detached flat plates, drag and lift coefficients, Reynolds numbers, square cylinder, Strouhal number.

I. Introduction

FLOW over bluff bodies plays an important in practical engineering applications. Most of the work on bluff bodies is related to the study of flow induced vibrations, their resulting effects on the structures, dependence of wake patterns and aerodynamic force characteristics on different parameters [1]-[3]. Many applications of bluff bodies can be found in road vehicles, cooling towers, cable suspension bridges, high-rise buildings, heat exchangers, and energy savers at higher Reynolds numbers ($Re = U_\infty d/\nu$, U_∞ is inflow velocity, d is size of an object and ν is the kinematics viscosity), whereas at low range of Reynolds number, these applications can be obtained in the computer equipments and micro-electro-mechanical-systems (MEMS) etc. [1].

Shams-ul-Islam is with the Mathematics Department, COMSATS Institute of Information Technology Islamabad, 44000, Pakistan (corresponding author, Phone: 0092-3139840066; e-mail: islam_shams@comsats.edu.pk).

Raheela Manzoor is with the Mathematics Department, COMSATS Institute of Information Technology Islamabad, 44000, Pakistan (e-mail: raheela_manzoor@yahoo.com).

Zhou Chao Ying is with the Shenzhen Graduate School, Harbin Institute of Technology, Shenzhen University Town, Shenzhen China, 518055 (e-mail: cyzhou@hit.edu.cn).

The geometry of bluff body is simplest but it has complex flow structure in near wake. It is essential to investigate the flow structure when near wake is interfered with a flat plate. Because of that, all-inclusive understanding about flow structure mechanism can be obtained at a great extent. The researchers developed different methods to achieve better flow control in order to suppress the vortex shedding behind the main object and to reduce the magnitude of drag and lift force that may cause structural damage under some antagonistic conditions [1]. Among these methods, one of the methods is known as passive control method. This method controls the vortex shedding by transmogrifying the shape of bluff body or by attaching some devices in flow stream. Much of the literature based on passive control methods.

Roshko [1] carried out experimental study to suppress the vortex shedding for flow past a circular cylinder with detached flat plate at downstream location. He found that $g \approx 2.7$ (g is the spacing between circular cylinder and flat plate) is a critical gap spacing, where vortices suppressed completely and Strouhal number ($St = f_s d/U_{max}$, f_s is vortex shedding frequency) diminishes.

Apelt et al. [2] experimentally examined the effect of detached flat plate placed downstream to a circular cylinder in order to control the vortex shedding. They studied different Reynolds numbers. They investigated that if the length L = 1d, then drag force will be reduced and attain its minimum value, whereas St will also be decreased. Furthermore, Apelt and West [3] experimentally introduced constant drag coefficient with no vortex shedding by using the length of control plate L > 5d.

Sakamoto and Hanui [4] conducted an experiment for reduction of fluid forces. They examined different stream wise arrangement of main circular cylinder and control cylinder and observed maximum reduction at $Re = 6.5 \times 10^4$ in root mean square value of drag (Cdrms) and lift (Clrms) coefficients. The effect of control plate at near wake of semicircular cylinder was studied experimentally by Boisaubert and Texier [5]. They used Re = 200 and 400 and deduced the generation of secondary vortices in recirculation zone.

Ozono [6] conducted an experimental study for flow past a rectangular and circular cylinder. He put a thin splitter plate downstream to the cylinder and examined complete vortex suppression. Igarashi [7] experimentally observed two different flow behaviors at $Re = 30 \times 10^3$ with and without vortex shedding. These behaviors depend on the transverse distance and diameter of the control plate and found a critical

gap (g_c) at which the transition occurred. For gap spacing $g > g_c$, there would be a decrease in St and it increases when $g \leq g_c$. He pointed out that when $g \leq g_c$, the maximum reduction in drag occurred. A study on semi-circular cylinder with a downstream flat plate of chord length is also done by Farhadi et al. [8]. They investigate different phenomena for Re ranging from 100 to 500 at fixed g. They calculated the critical gap spacing g_c = 4.6d where maximum reduction in fluid forces occurred. Further, they concluded that the critical gap spacing for this configuration is larger than a critical gap spacing of circular cylinder which is g_c = 2.6d. One can also find some numerical investigation for fluid forces reduction.

Kwon and Choi [9] conducted numerical simulation study to find out the effect of detached flat plate on vortex shedding behind a circular cylinder with respect to Re and L (L = length of plate placed at downstream of main cylinder). They deduced that the vortices disappeared throughout the computational domain is related to Re. Islam et al. [10] numerically examined that gap spacing from 2d to 2.5d is the critical gap spacing, where the force statistics reach either maxima or minima. As a result, the shed vortices behind the detached flat plate are also affected. They studied the force reduction and flow patterns for detached flat plate at the downstream position.

Turki [11] numerically found the vortex shedding using a control volume finite element method. He used detached flat plate behind a square cylinder for Reynolds number ranging from 110 to 200 and investigated that St increases as g increases and approaches to single cylinder value without flat plate. Furthermore, he found that at Re = 200, St decreases as by increasing g and reaches to its minimum value at g = 2.82d. Islam et al. [12] numerically examined the reduction of fluid forces using the control plate in detached configuration for various gap spacing and Reynolds numbers using the lattice Boltzmann method. They investigated the critical gap spacing at g = 2d - 2.25d, where the maxima or minima in physical parameters exist and they classified the flow behavior into three different regimes on the basis of small, moderate and high gap spacing.

Alam et al. [13] investigated suppression of fluid forces acting on two tandem square cylinder in presence of thin plate by taking Re = 56000 and found maximum reduction on mean and fluctuating forces occurs. A numerical study on fluid force reduction acting on a square cylinder in presence of downstream control plate is carried out by Zhou et al. [14] using a parabolic velocity profile at inlet of channel. They varied the length of control plate from 10% to 100% of cylinder width and gap spacing from 0.5d to 3d of cylinder width and not found drag reduction.

Ali et al. [15] reported the effect of control plate lengths on square cylinder with fixed Re of 150 through Open FOAM numerical simulation system based on finite element method. They obtained three flow regimes depending upon length of control plate in their study: (i) for $L \leq d$, (ii) for $1.25d \leq L \leq 4.75d$, (iii) for $L \geq 5d$ and found that most appropriate length is $L \leq 4d$. Sohanker et al. [16] conducted a numerical study on fluid force reduction for flow past a square cylinder in presence of upstream flat plate using volume code based on SIMPLEC algorithm at Re ranging from 50 to 200. They found maximum reduction in fluid forces at g = 3d and Re = 160. Furthermore, they identified three types of flow regimes. The vortex shedding completely suppressed in regime I and II.

Gupta [17] numerically examined the reduction of vortex shedding using splitter plate in the wake of cylinder by direct numerical simulation (DNS) by taking the width of control plate 0.2d which controlled the flow around the cylinder at $\mathrm{Re} = 100$. He also observed that on the edge of cylinder where shear layer separates and control plate ashore, the complete vanishing of vortex shedding. Furthermore, he also pointed out that the reduction of drag force on the main cylinder was also due to the suppression of vortex vortices.

Hawang and Yang [18] studied the significance of two splitter plates with same length as diameter of circular cylinder. One is placed at upstream location and second one is placed is downstream location of circular cylinder in order to reduce drag force by using finite volume method. They examined that both plates play a vital role to reduce a drag; the upstream plate reduces pressure with secondary effect of increasing base pressure, while the downstream one suppress the vortices. The maximum drag reduction is observed at g_1 = 1.5d and g_2 = 2.4d that is 38.6% (where g_1 is surface to surface distance from upstream plate to main cylinder and g_2 is surface to surface distance from main cylinder to downstream plate). Lu et al. [19] numerically examined the fluid flow past a circular cylinder with multiple control rods and systematically studied the VIV suppression mechanism under the influence of gap spacing, rods and cylinder diameter ratio, Reynolds number, number of control rods and angle of attack on hydrodynamics of main circular cylinder. They identified four different flow regimes on the basis of drag and lift reduction. Also, they observed that drag and lift coefficients are increased slightly compared with right angle of attack ($\theta = 0$). The peak frequency of drag coefficient decreases by increasing angle of attack. Furthermore, their results shows that use of six control rods gives better performance in force reduction of man cylinder than using one, three or four control rods. Vamsee et al. [20] numerically examined the effect of a single splitter plate present at upstream location and presence of upstream and downstream splitter plates for low Reynolds numbers using finite difference discretization and MAC algorithms. They found that upstream plate has a vital role in drag reduction but has less effect in stabilizing the flow behind the cylinder. For upstream location of splitter plate, percentage reduction in drag force occurred was about 27% and for the case of fixing upstream plate by varying the length and gap spacing between the downstream plate and cylinder, the drag reduction obtained was 35%. From above mentioned literature, it is clear that a little attention is paid to investigate the effect of Reynolds number on flow past a square cylinder in presence of upstream flat plate and comparison of drag reduction obtained due to presence of upstream fat plate and downstream flat plate alone at different Reynolds numbers. Main objective of this work is to find the effect of Reynolds number on flow characteristics and to reduce drag force due to

passive control method by putting flat plates at upstream and downstream locations of main cylinder at fixed length of plate (L = 4d) and small gap spacing g = 0.5d - d between the cylinder and flat plate.

This paper is organized as follows. After the introduction in Section I, problem description and boundary conditions are given in Section II. In Section III, we presented the results and discussions. Finally, conclusions are drawn in Section IV.

II. Problem Description and Boundary Conditions

Figs. 1, 2 show a two-dimensional computational domain consists of flat plates of length 'L' and square cylinder of size d (confined between the channel walls.). In first case, a flat plate is placed at upstream position of cylinder, while in other one flat plate is placed at downstream position of main cylinder. L_u is the upstream position from inlet to flat plate, L_d is the distance from the downstream flat plate to exit of the computational domain, h is the width of the splitter plate, L_x is the length and H is the height of the computational domain, respectively. Due to the confined flow the velocity profile we adopted here is parabolic ($u = 1.5U_\infty(1-(y/h)^2)$, where y is the vertical distance from the centerline and U_∞ is the mean flow velocity). The length of plate is fixed for both configurations. In the experimental study, done by [3]; it was observed that the maximum flat plate thickness up to 10% of cylinder diameter could be taken for longer plates without edge effect making any significant contribution. Therefore, thickness of control plate taken here is 0.1d. The gap spacing between the plate and cylinder is chosen from g = 0.5d to 1d at to study the effect of Reynolds number having the range from 80 to160. The higher range of Re converts the flow into three dimensional as proposed by [23] and [24].

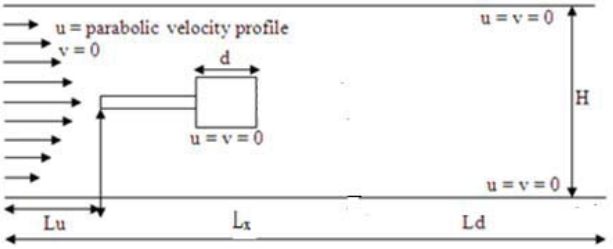

Fig. 1 The schematic flow configuration for upstream flat plate

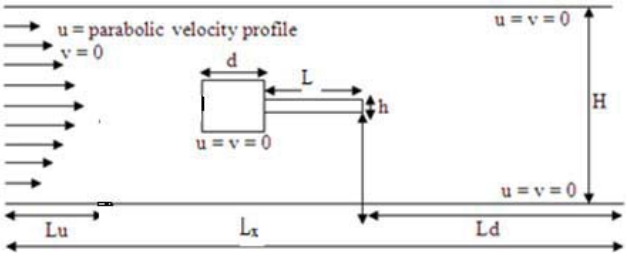

Fig. 2 The schematic flow configuration for downstream flat plate

The no-slip (**u = v = 0**) boundary conditions are used at the surfaces of the square cylinder and flat plates [26], as well as at top and bottom walls of channel, while the convective boundary conditions are applied at the exit of the computational domain [25]. To investigate the effects of force statistics on main cylinder, the drag and lift coefficients are defined as $Cd = \frac{2\,F_d}{\rho U_\infty^2 d}$ and $Cl = \frac{2\,F_l}{\rho U_\infty^2 d}$. The force $\mathbf{F_d}$ acting in stream-wise **x** direction and $\mathbf{F_l}$ acting in transverse directions respectively. The gap spacing between the flat plate and cylinder in dimensionless form is defined as $g = \frac{s}{d}$, s is surface to surface distance between the cylinder and flat plate. The hydrodynamic forces on the control plate and square cylinder are calculated using the momentum exchange method [27]. All the computations are carried out on an Intel® Core™ i5-2450M CPU @ 2.50GHz processor and 8GB RAM. Different values of relaxation parameters on different Reynolds numbers are shown in Table. I.

TABLE I
Values of Relaxation Parameters

Reynolds number (Re)	Uniform inflow velocity (U_∞)	Single relaxation-time parameter (τ)
80	0.043859649122807	0.532894736
100	0.043859649122807	0.526315789
120	0.043859649122807	0.521929824
140	0.043859649122807	0.518796992
150	0.043859649122807	0.517543859
180	0.043859649122807	0.514619883
200	0.043859649122807	0.513157894

One can find more detail about the lattice Boltzmann method, grid independence, effect of computational domain and some more interesting observations in [28]-[34].

III. Results and Discussions

The effects of Reynolds number on fluid force reduction and suppression of vortex shedding flow past a square cylinder in presence of upstream and downstream flat plate alone are discussed by taking small gap spacing g = 0.5d and 1d at fixed length of flat plate L = 4d using single-relaxation-time lattice Boltzmann method (SRT-LBM). The variation of Reynolds number is chosen from 80-200. Wake structure mechanism, time signal analysis of drag and lift coefficients and power spectra analysis of lift coefficients are discussed. The variations of physical parameters obtained in presence of flat plates are compared with force coefficients of single cylinder. The obtained results are divided into two sections. In first section we will discuss the effects of Re in presence of downstream flat in the form of flow field behavior and analysis of force statistics. Similarly, in second section we will discuss Re effects due to presence of upstream flat plate.

A. Downstream Flat Plate

In order to study the effect of Reynolds on flow structure mechanism and reduction of fluid forces, a flat plate is used at downstream position of square cylinder having diameter 4d in detached configuration by taking gap spacing g = 0.5d and 1d. The Reynolds number is varied from 80 to 200. Typical wake pattern in terms of vorticity plots for different Reynolds

number are shown in Figs. 3 (a)-(d) for chosen both gap spacings. The variation of drag and lift fluctuations against time and corresponding power spectra analysis of lift coefficients are plotted in Figs. 3 (a)-(e) and 5 (a)-(e). Two types of flow patterns were observed, named as (i) SFpattern, (ii) SLRpattern. At small Reynolds number that is from 80-120 flow does not generate any vortices, steady stream lines form into whole computational domain for g = 0.5d and d. After increasing Re as shown in Figs. 4 (b), (d), (e), an alternate vortex shedding is observed behind the detached flat plate for all chosen Reynolds number. The shear layer generated from main cylinder reattaches with flat plate, rolled up and transform into vortices that travel downstream in an alternate manner. The length of vortex formation reduced as Re increases. The strength and size of vortices shed at near downstream position is also different. The number of vortices increases with the increment in Reynolds number. We also observed that the length and width of shed vortices near flat plate reduced by varying Reynolds number. At high Reynolds number, vortices spread throughout the computational domain and greatly effect on upper and lower wall as well as compared to small and moderate Reynolds number as shown in Fig. 4. Due to small gap spacing, we did not observe any vortices between the gap. It is because shear layer generated from cylinder quickly reattach to flat plate. This SLRflow regime also occurred in [22], [11] and [12]. The flow behavior can also be seen from streamline graph (Figs. 4 (a)-(e)). For SFbehavior no separation zone developed. Streamlines travel downward in wavy form. For moderate and high Reynolds number, separation zone formed, which assured the existence of alternate vortices travelling towards downstream position. As changing the Re, separation vortex also changed its position and became wider for large Reynolds number. Two bubbles can be visualized in streamlines graph, which assures the existence of symmetric flow behavior between the gaps. Figs. 5 (a)-(e) show time trace analysis of drag and lift coefficients. The drag coefficients represent a constant behavior at all Reynolds numbers. The magnitude of drag coefficient having negative values at g = 1d and Re = 120, because of adverse pressure. The lift coefficients having a periodic behavior for unsteady flow pattern at Re $\geq$ 120 and having constant nature for SFpattern. The magnitude of drag and lift coefficients both increases as Reynolds number increases. The power spectra analysis of lift coefficients represents a sharp single peak without any secondary frequency. Because no modulation in lift coefficients generated, only an alternate vortices generated and travelled downward. The magnitude of power spectra increases with increase in Reynolds number. For high Reynolds number, sharp peak transformed into broad banded peak.

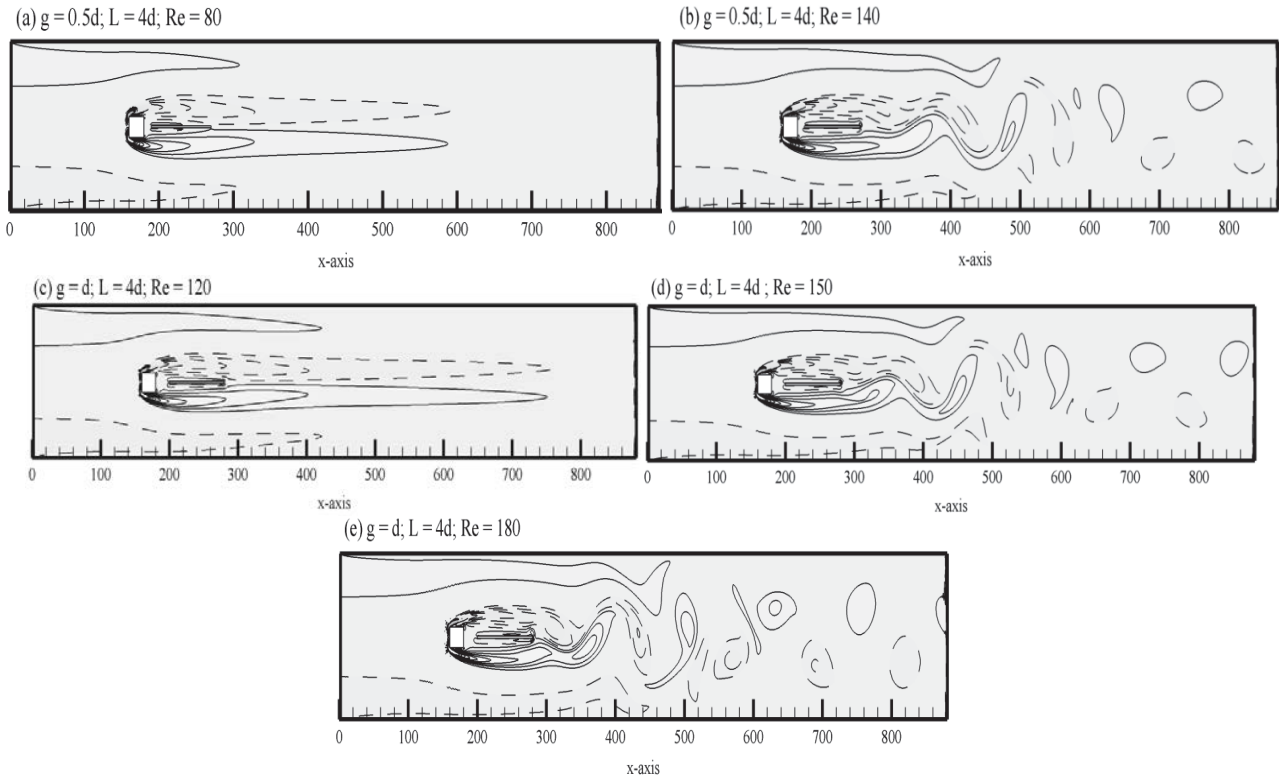

Fig. 3 Vorticity contours visualization for flow past a square cylinder with downstream flat plate at different Reynolds number

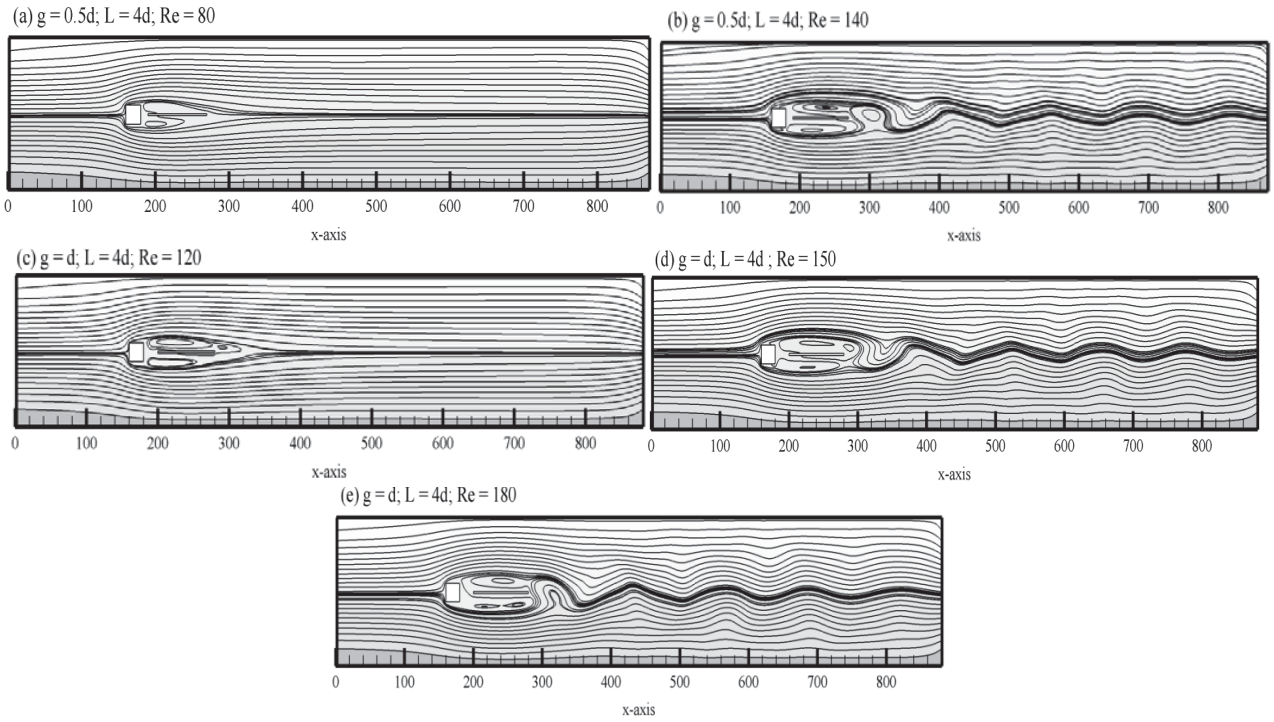

Fig. 4 Streamlines visualization for flow past a square cylinder with downstream flat plate at different Reynolds number

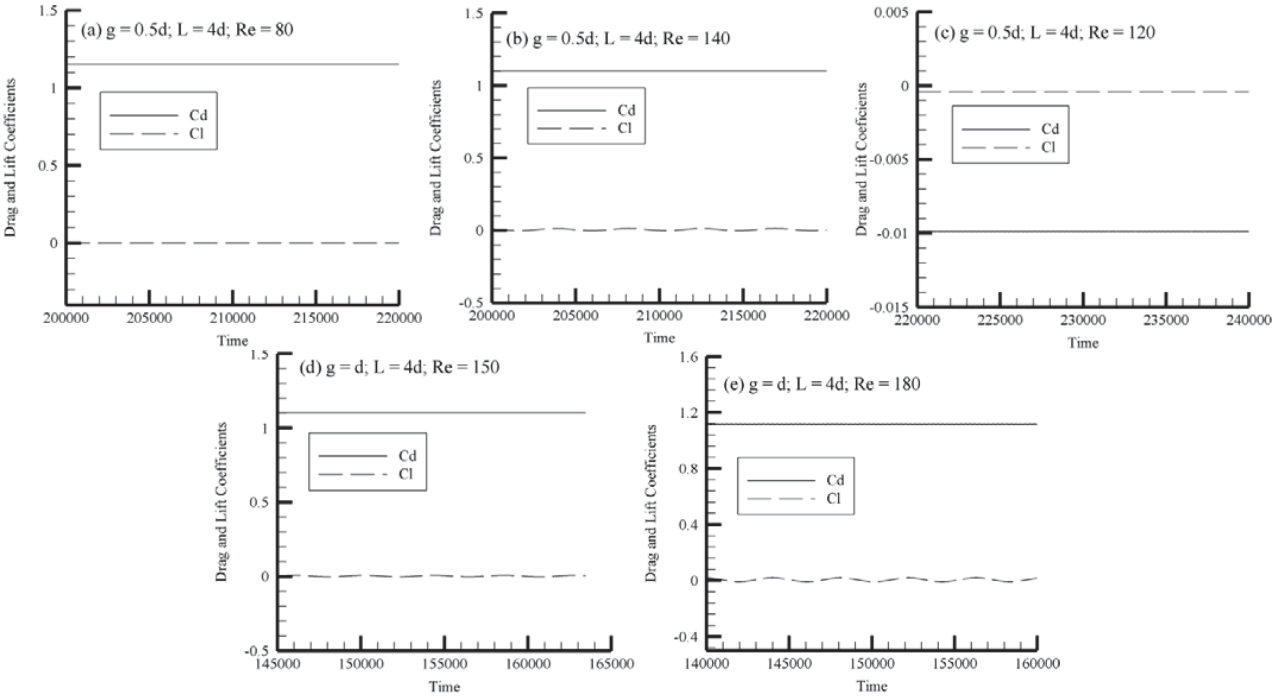

Fig. 5 Time trace analysis of drag and lift coefficients for flow past a square cylinder with downstream flat plate at different Reynolds number

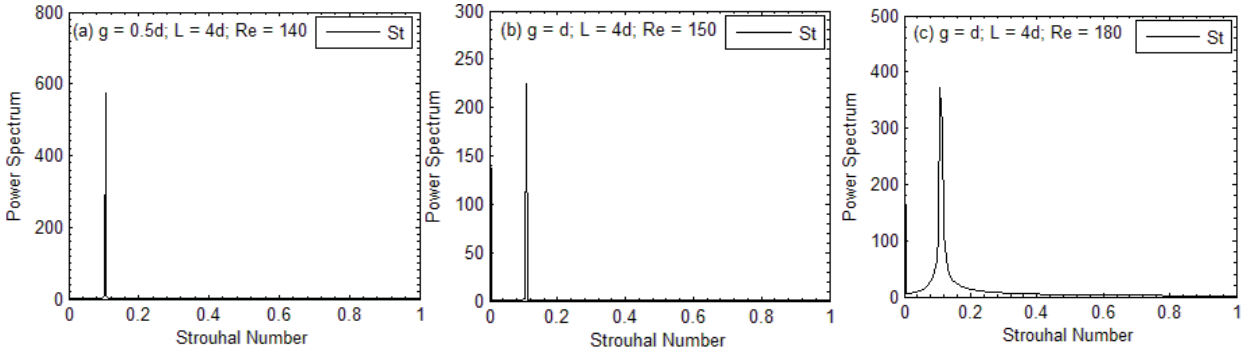

Fig. 6 Power spectra analysis of drag and lift coefficients for flow past a square cylinder with downstream flat plate at different Reynolds number

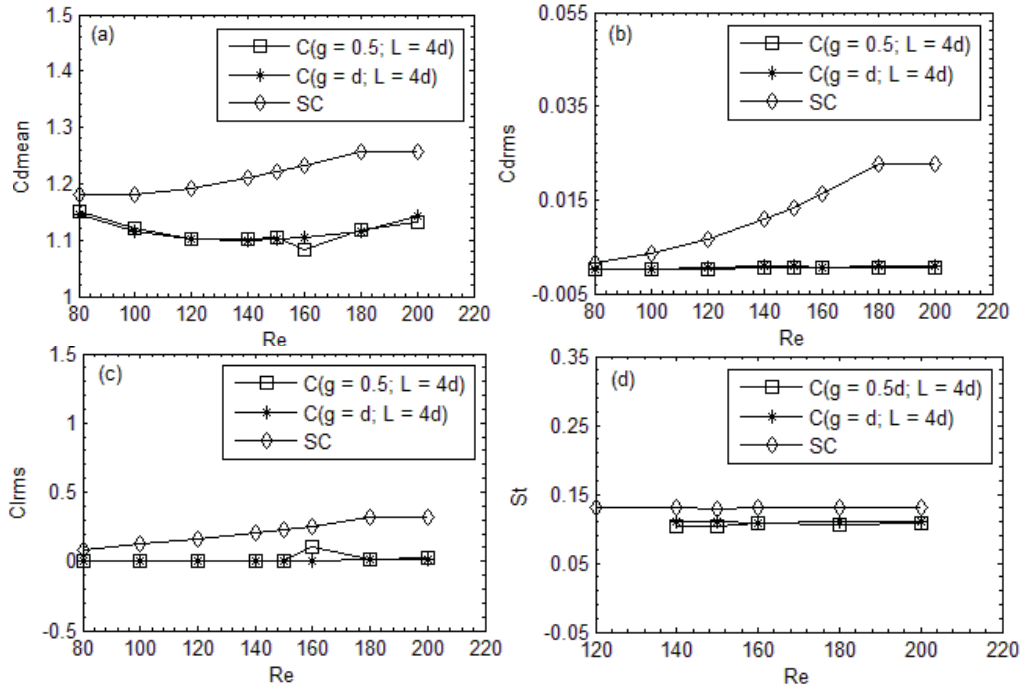

Fig. 7 Variation of (a) Cdmean (b) Cdrms (c) Clrms (d) St for flow past a square cylinder with downstream flat plate at different Reynolds number

The data of physical parameters of present results are plotted versus Reynolds number in Figs. 7 (a)-(d) and 8 (a)-(c) together with single cylinder data for comparison. It can be observed that present results show minimum values than single cylinder for all physical parameters such as mean drag coefficients, root mean square value of drag and lift coefficients and Strouhal number. The value of Cdmean first decreases up to Re = 140 then showing increasing behavior for $140 \leq Re \leq 200$; here flow pattern changes from steady to unsteady flow pattern. The mean drag coefficient of single cylinder has increasing trend with increasing Re till 180, then remain almost constant at Re = 200. The maximum value of Cdmean occurred at Re = 80 for detached flat plate case at g = 0.5d, that is 1.1502. The existing flow pattern here is in steady state. No vortices appear between the gap as well as downstream positions of flat plate. The root mean square values of drag and lift coefficients are smaller than that of single cylinder for both chosen gap spacing at fixed length of flat plate. For g = 1d, Cdrms increases with the increasing Re, but at g = 0.5d, it represents an irregular behavior some time increasing or decreasing. But, this increment or decrement is small that is almost negligible. The maximum Cdrms value is 0.001 at g = 1d and Re = 140.The root mean square value of lift coefficients have constant behavior and almost same values at $80 \leq Re \leq 120$, because here no lift force exists. Flow behaves as a steady streamlines. After Re > 140, Clrms start to be increase due to alternate generation of vortices (Fig. 7 (c)). The root mean square value of single cylinder is maximum than root mean square values of detached flat plate with cylinder. The power spectra analysis of lift coefficient is shown in Fig. 7 (d). Unsteady flow exists for $Re \geq 120$. The values of St for single cylinder is little bit greater than other

cases of flat plate. It represents increasing or decreasing for Re≥ 120 at g = 0.5d, but for g = d, St remains constant as Reynolds number increases. It is because of the reason that vortex shedding frequency almost remains same at higher Reynolds number. The maximum value of St is 0.1108 at Re = 200 and g = d, where strong interaction between the vortices exist, and flow remain critical near downstream position of flat plate.

The average values of physical parameters are shown in Figs. 8 (a)-(c). The average Cdmean first decreases till R = 140, then increases for both chosen gap spacing. A jump can also be seen in Cdmean between Re = 140-180 for g = d. At that values of Re the vortex shedding frequency increases and strong vortices generated at downstream of flat plate. The maximum value of average Cdmean is 1.12 at g = 1d and Re = 160. The average value of root mean square values of drag and lift coefficients for g = 0 and d having increasing trend with increment in Re. The maximum increase starts to occur at Re ranging from 140-200. Whereas Cdrms and Clrms for g = 0.5d increases or decreases with Re. A jump can also be observed at Re = 160, where maximum fluid forces occurred. Maximum average root mean square values of drag and lift forces that are 0.00062153 and 0.0286 also occurred at Re = 200 and g = 0.5d. The percentage reduction in mean drag coefficients and root mean square values of drag coefficients for both gap spacing at different Reynolds numbers are shown in Figs. 9 (a), (b). The reduction in Cdmean increases first by increasing Re, approaches to maximum reduction at (g, Re) = (1d, 180) that is 11.10%, then decreases. The percentage reduction in Cdrms increases or decreases with Reynolds number. The maximum reduction in Cdrms is 97.6% at Re = 180 and g = 0.5d, where SLRflow pattern exists. Thus, present results show that the force coefficients are reduced significantly by using the flat plate in downstream position of square cylinder and suppression of vortices also exists at small Reynolds number.

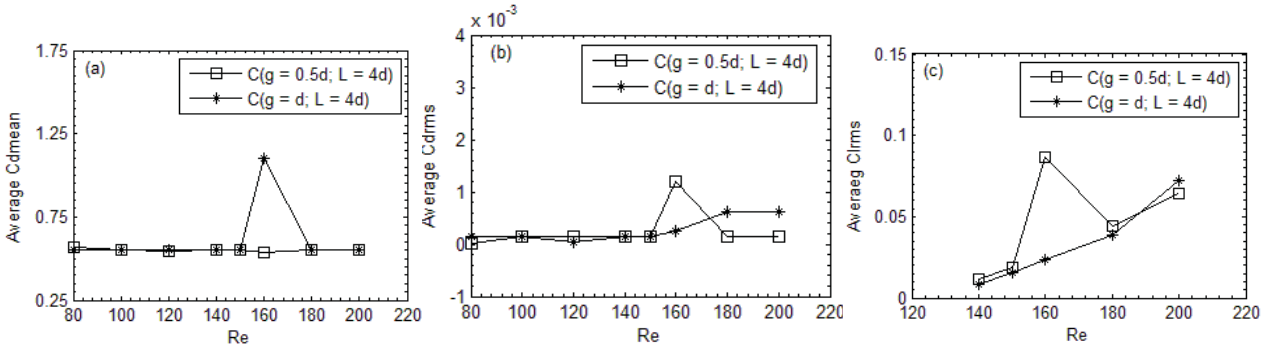

Fig. 8.Variation of Average (a) Cdmean (b) Cdrms (c) Clrms for flow past a square cylinder with downstream flat plate at different Reynolds number

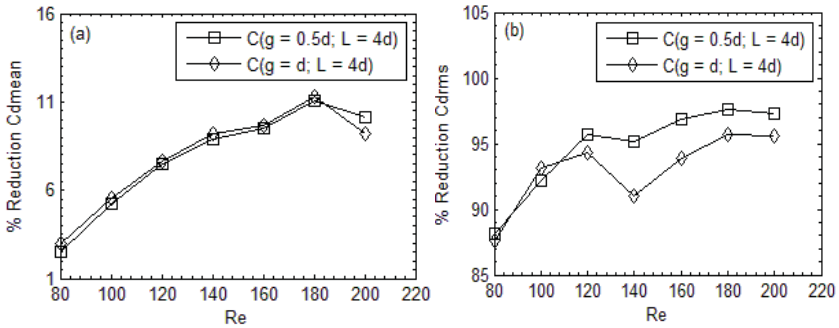

Fig. 9 Percentage reduction in (a) Cdmean (b) Cdrms for flow past a square cylinder with downstream flat plate at different Reynolds number

B. Upstream Flat Plate

The effect of Reynolds number on flow past a square cylinder in presence of upstream flat plate of length L = 4d with gap spacing g = 0.5d, d are investigated in this section. The range of Reynolds number is chosen from 80-200 to study the flow behavior and reduction of fluid forces. The acquired results are in the form of vorticity contour visualization, time trace analysis of drag and lift coefficients and energy spectrum. Some physical parameters are also computed to find the behavior of fluid forces such as Cdmean, Cdrms, Clrms and St. Figs. 10 (a)-(f) show a wake structure mechanism in terms of vorticity contour. Two different types of flow pattern have been found, named as (i) QSF, (ii) SBB. At low Reynolds number, flow is nearly unsteady; as the Reynolds number increases, vortices start to be appeared near the cylinder as well into whole computational domain. The effect of vortices also felt at upper and lower walls of domain. In both selected gap spacing g = 0.5d, the shear layer emerging from upstream flat plate moves toward the cylinder without causing any disturbance in flow. This shear layer is rolled up

at near downstream and transformed vortices which travelled downward in an alternate way. The Reynolds number increases wake formation length next to cylinder reduces and width increases. Also, the size and strength of vortices enhanced with increasing Reynolds number, that is clear from Fig. 10. The Re = 80 is considered as a critical Reynolds number, a drastic change in flow pattern occurred here. For case g = 1d, a steady stream formed between the gaps due to passing the flow, but no flow can be seen between the gap for g = 0.5d due to negligible gap spacing. In comparison of gap spacing with different Reynolds number, the size of vortices changes by increasing g. The higher range of Reynolds number developed higher magnitude of lift coefficients as compared to low range of Reynolds number. The flow structure mechanism also can be seen from streamlines graph (Figs. 11 (a)-(e)). For Re = 80, no separation zone observed downstream which assures the steady streamlines near downstream position due to existence of small eddies near the cylinder. As the increment in Reynolds number hold, the separation zone developed because of an alternate generation of vortices.

The time trace analysis of drag and lift coefficients are given in Figs. 12 (a)-(e). The drag coefficients represent a constant behavior for Re ≤ 120. As vortices strengthen and change their size due to increasing Reynolds number, a periodicity seem to be observed in drag for $120 \leq Re \leq 180$. At higher Reynolds number Re = 200, shear layer reattaches to cylinder and attains a complex structure and as a result drag have modulated behaviour. The magnitude of drag increases from Re = 100 to 180 whereas lift coefficients have periodicity for all Reynolds number due to an alternate generation of vortices. Its magnitude also depends on Reynolds; increases by increasing Re. The power spectra analysis has a sharp single peak due to existence of only primary frequency (Figs. 13 (a)-(i)). The frequency of power spectra increases with increasing Reynolds number, but decreases with increasing gap spacing.

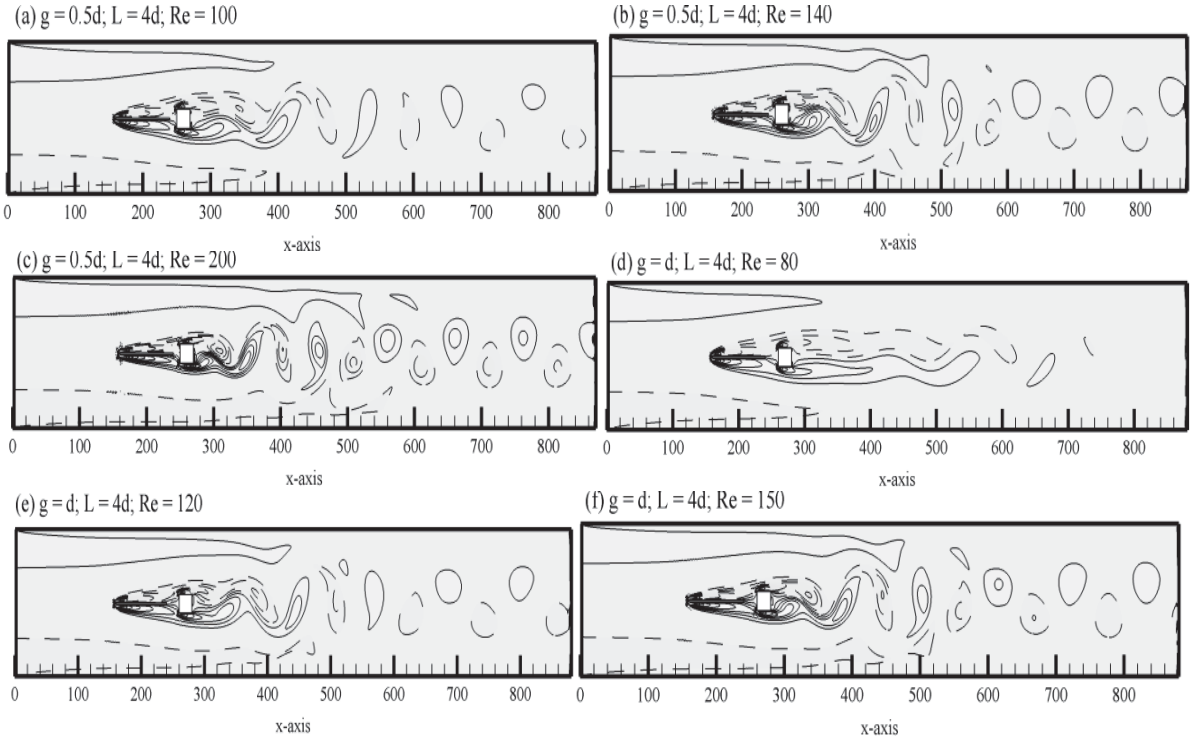

Fig. 10 Vorticity contours visualization for flow past a square cylinder with upstream flat plate at different Reynolds number

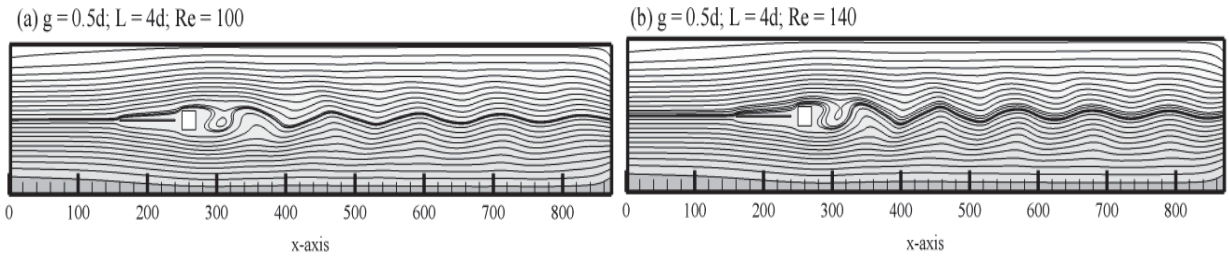

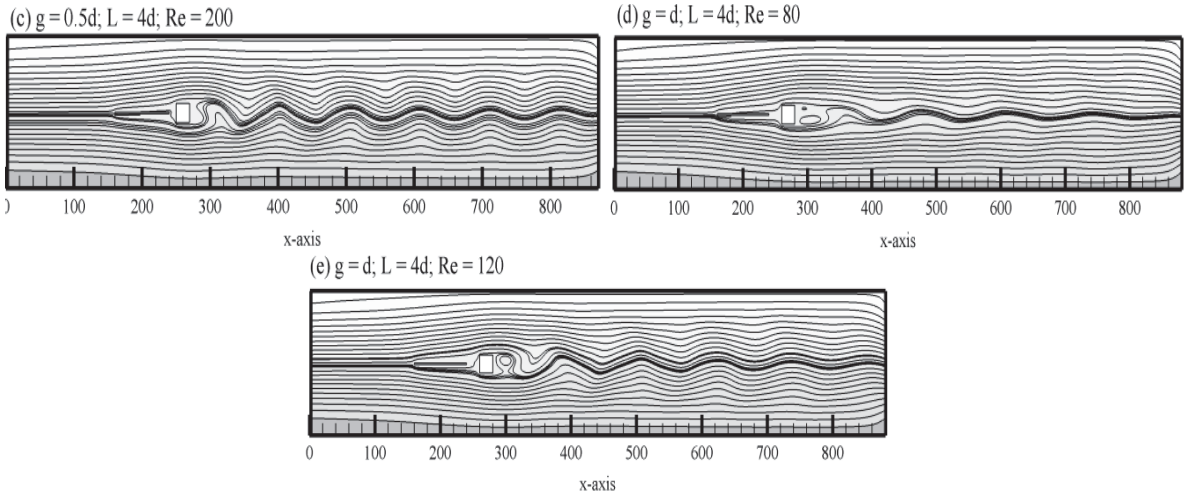

Fig. 11 Streamlines for flow past a square cylinder with upstream flat plate at different Reynolds number

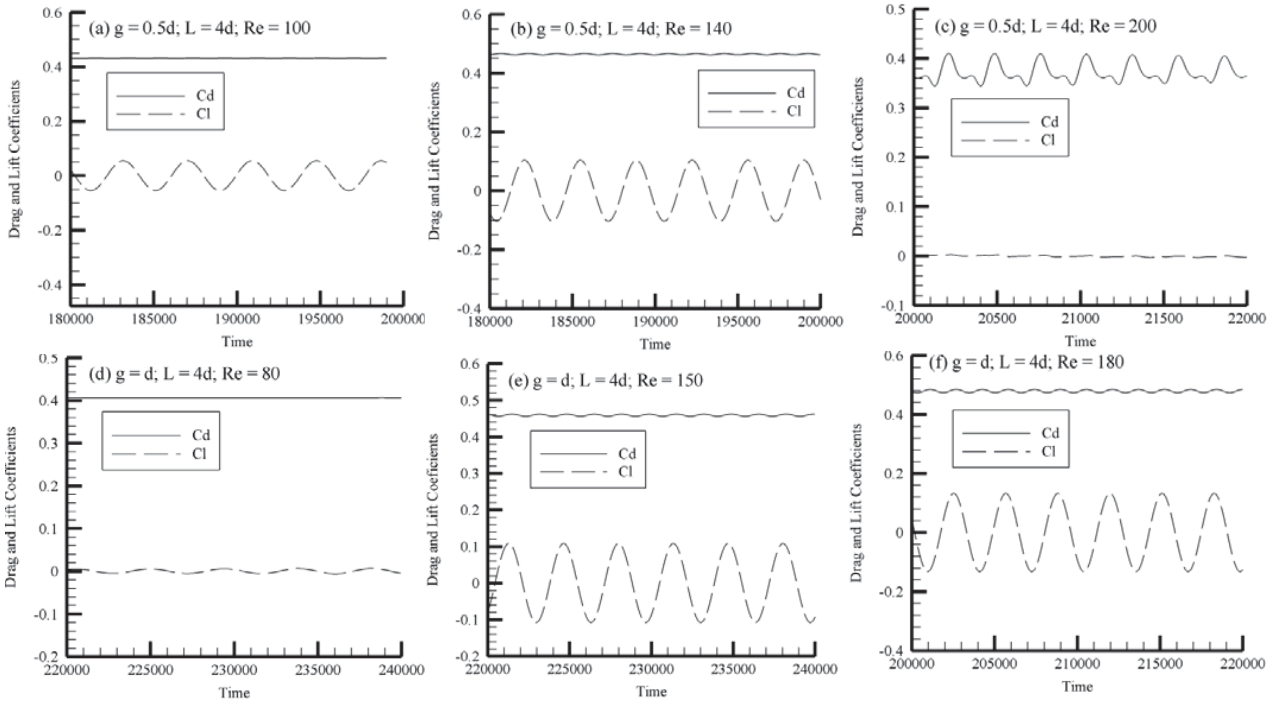

Fig. 12 Time trace analysis of drag and lift coefficients for flow past a square cylinder with upstream flat plate at different Reynolds number

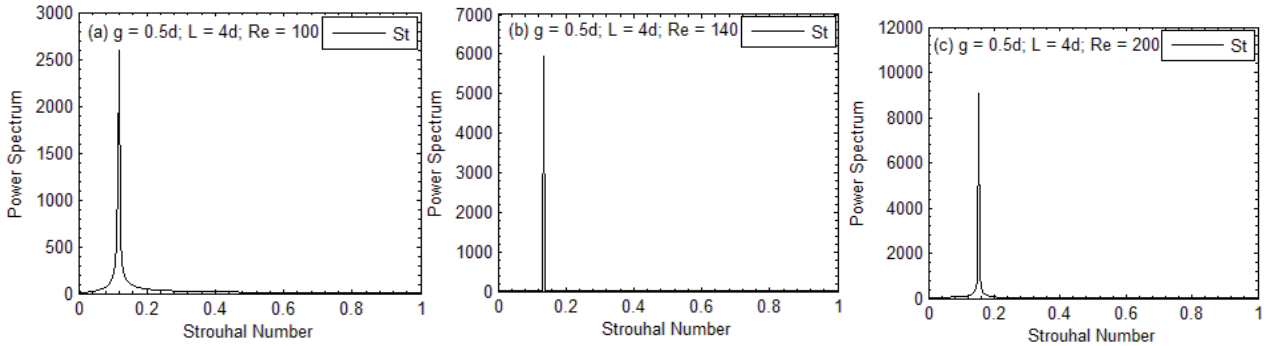

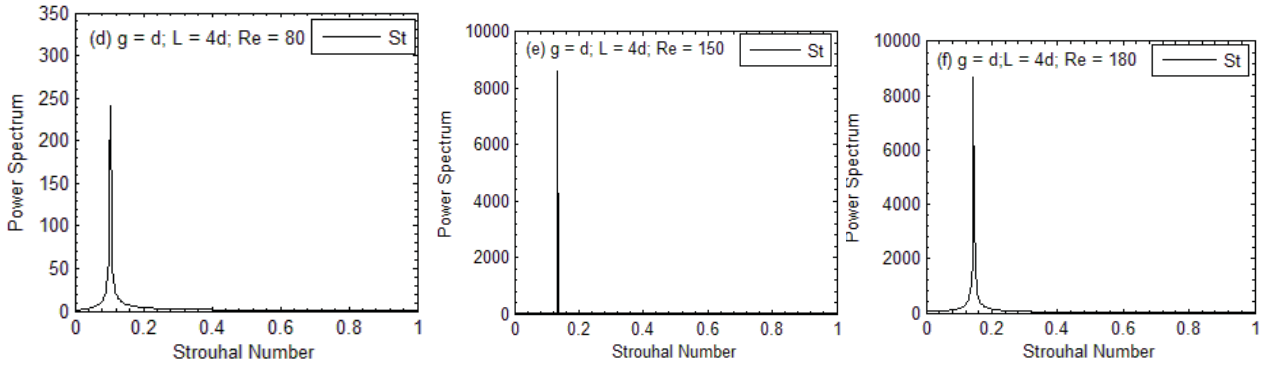

Fig. 13 Power spectra analysis of drag and lift coefficients for flow past a square cylinder with upstream flat plate at different Reynolds number

The variation of aerodynamic force coefficients and reduction in aerodynamic force with Re at different spacing values is presented in Figs. 14 (a)-(d), 15 (a)-(c). The Single cylinder values are also plotted in the graphs for comparison. It can be observed that the Cdmean of cylinder for both chosen gap spacings is less than those of Single cylinder values at all Re in the spacing range 0.5d-1d. The values of Cdmean strictly increases with increasing Re for both g, reason to increase Cdmean continually is that we observe vortices as compared to Re = 80. The gap spacing g = 0.5d contains larger values of mean drag force than g = 1d. It means that when flat plate is close to cylinder, it disturbed the flow in a great extent than large spacing. The maximum Cdmean value is 0.5094 at (Re, g) = (200, 0.5d), where we obtained complex flow structure near main cylinder and modulated drag coefficients. Like Cdmean, Cdrms and Clrms of cylinder in presence of upstream flat plate is less than Single cylinder values except at Re = 80 and 100, where Cdrms of Single cylinder is close to cylinder's Cdrms with flat plate present at upstream location. The Cdrms has increasing and decreasing trend with increasing all Reynolds number, while Clrms strictly increases with increasing Re, because as Re increasing, the shedding frequency increases which strengthens the vortices and root mean square values of lift coefficients enhanced. The maximum value of Cdrms and Clrms is 0.0059 and 0.1141 at (Re, g) = (200, 0.5d). In short, we can say that small gap spacing with high Reynolds number produced much aerodynamics forces than high gap spacing with small Reynolds number. The St values are shown in Fig. 14 (d), which are less than single cylinder values for Re <140 except g = 0.5d that attains larger St at Re = 80. As Reynolds number increases from 140, then single cylinder St decreases as compared to square cylinder in presence of flat plate. At high Reynolds number, the influence of flat plate on square cylinder, which enlarge the magnitude of vortex shedding frequency. As a result, St values increases as compared to single cylinder St value. The maximum value of St occurred at 0.1507 at (Re, g) = (200, 1d).

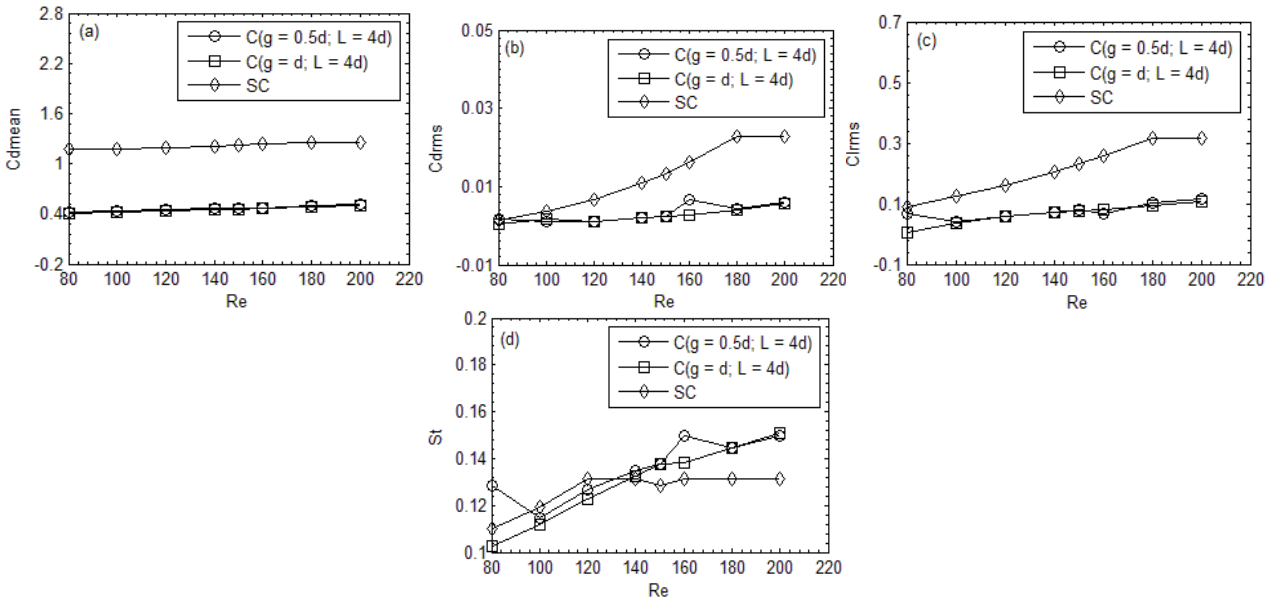

Fig. 14 Variation of (a) Cdmean (b) Cdrms (c) Clrms (d) St for flow past a square cylinder with upstream flat plate at different Reynolds number

The dependence of average values of physical parameters on Reynolds number is shown in Figs. 15 (a)-(c). The average value of mean drag coefficients increases with increment in Re for g = d, but at g = 0.5d, average value of mean drag force first decreases at Re = 100 then increases up to Re = 200. The maximum value of average Cdmean is obtained at (Re, g) = (200, 0.5d) that is 0.2684. The average root mean square value of drag coefficients has mixed trend decreasing or increasing. For both gap spacings, it reduced from Re = 100-120 after that it started to increase except for g = 0.5d and Re = 160 in which it showed a jump. This jump basically represents transition in flow pattern. The maximum average value of Cdrms is 0.0055 at (Re, g) = (200, 1d). Like Average Cdmean, average Clrms also has increasing trend with respect to all selected Reynolds number for g = 1d but for g = 0.5d, average Clrms decreases at Re = 100 then starts to increase up to Re = 200 and approaches to its maximum value 0.1141 at (Re, g) = (200, 0.5d). In order to check the reduction in aerodynamics fluid forces due to presence of flat plate, a percentage reduction in Cdmean and Cdrms is computed against Re as shown in Figs. 16 (a), (b). The percentage reduction in Cdmean decreases with increase in Re. It is due to high mean drag force at large value of Reynolds number. The gap spacing g = 0.5d attains maximum reduction at Re = 80, that is 89.1%, the reduction about 59.5% observed at (Re, g) = (200, 0.5d The reduction in root mean square value of drag force shows increasing or decreasing with increment in Re. The percentage reduction in Cdrms for all chosen g decreases at small values of Re that are 80-120, then increases till Re = 140-160. At the end at high Re value 180-200 again it becomes minimum. The maximum reduction in Cdrms is 86.3% at (Re, g) = (120, 1d). Fig. 17 presents the observed flow patterns.

IV. Conclusion

Two dimensional numerical simulations were performed to investigate the effect of Reynolds number (Re) on reduction of fluid forces for flow past a square cylinder in presence of single upstream flat plate and downstream flat plate. A two-dimensional numerical code is developed using SRT-LBM. First of all, code is validated for the flow past a square cylinder in absence of flat plate at different Reynolds number. The obtained results are compared to those available in literature and found to be in good agreement. After the validation, simulations were carried out first to find the effect of Reynolds number to control vortex shedding and in reduction of fluid forces at small gap spacing that are g = 0.5d and d at fixed length of flat plate L = 4d. The range of Reynolds number lies as $80 \leq Re \leq 200$. The achieved results of this study are mentioned below

1. Four different types of flow pattern were observed, two patterns for upstream flat plate location named as (i) QSF, (ii) SBB and two pattern for downstream flat plate location named as (i) SF, (ii) SLR.
2. For upstream flat plate location, significant drag reduction takes place but no suppression of vortex shedding observed.
3. For downstream flat plate location, suppression of vortex shedding examined at low Reynolds number for both chosen gap spacings. The flow remains steady at Re = 80-100 for g = 0.5d and 80 - 120 for g = d. Unsteadiness in flow seem to be exist at high range of Reynolds number Re > 120.
4. Mean drag force increases due to increasing Reynolds number for upstream flat plate case, but for downstream flat plate mean drag force representing a mixed trend increasing or decreasing through increasing Re.
5. For downstream flat plate case, Re = 140 is considered as a critical Reynolds number, where fluid forces may start to be increase or decreases. Re = 200 is the critical Reynolds number for upstream case.
6. The maximum reduction in mean drag force and root mean square value of drag force for downstream flat plate case is 11.10% and 97.6% obtained at (180, d) and (180, 0.5d).
7. The maximum reduction in mean drag force and root mean square value of drag force for upstream flat plate case is 89.1% and 86.3% at (80, 0.5d) and (120, 1d)

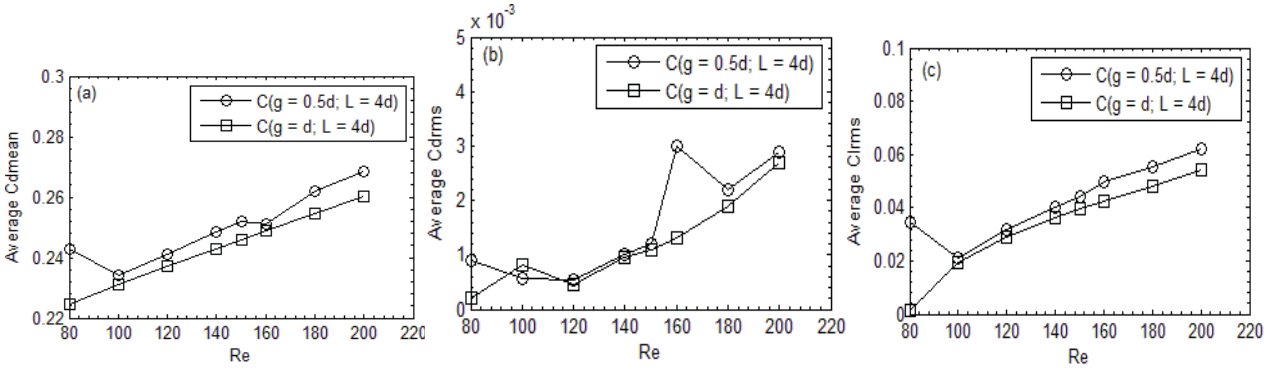

Fig. 15 Variation of Average (a) Cdmean (b) Cdrms (c) Clrms for flow past a square cylinder with upstream flat plate at different Reynolds number

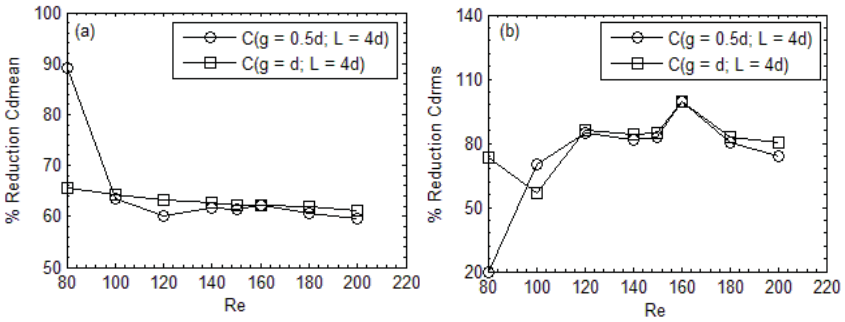

Fig. 16 Percentage reduction in (a) Cdmean (b) Cdrms for flow past a square cylinder with upstream flat plate at different Reynolds number

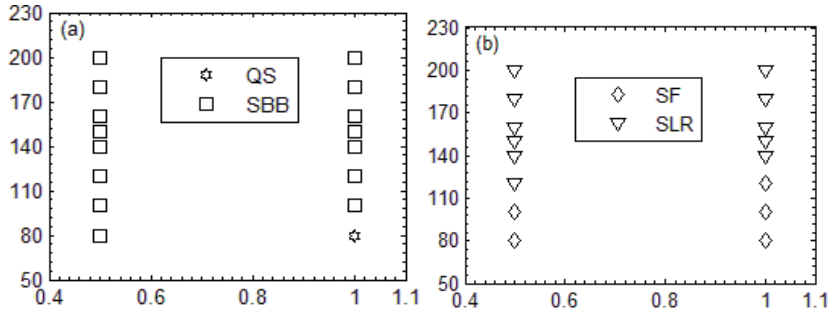

Fig. 17 Observed flow patterns for different Reynolds numbers due to presence of (a) upstream flat plate (b) downstream flat plate

REFERENCES

[1] A. Roshko, "On the drag and shedding frequency of two-dimensional bluff bodies," *National Advisory Committee for Aeronautics,* Technical note no. 3169.

[2] C. J. Apelt, G. S. West and A. A. Szewczyk, "The effects of wake splitter plates on the flow past a circular cylinder in the range $10^4 < R < 5 \times 10^4$," *Journal of Fluid Mechanics,* vol. 61, pp. 187-198, 1973.

[3] C. J. Apelt, G. S. West and A. A. Szewczyk, "The effects of wake splitter plates on the flow past a circular cylinder in the range $10^4 < Re < 5 \times 10^4$," Part 2, *Journal of Fluid Mechanics*, vol. 71, pp. 145-160, 1975.

[4] H. Sakamoto, K. N. TanTakeuchi, and H. Haniu, "Suppression of fluid forces acting on a square prism by passive contro," *Journal of Fluids Engineering*, vol. 119, pp. 506-511, 1997.

[5] A. Texier, A.S. Cruz Bustamante, L. David, "Contribution of a short separating plate on a control of a swirling process downstream a half-cylinder," *Experimental Thermal and Fluid Science,* vol. 265, pp. 565-572, 2002.

[6] S. Ozono, "Flow control of vortex shedding by a short splitter plate asymmetrically arranged downstream of a cylinder," *Physics of Fluids*, vol. 11, pp. 2928-2934.

[7] T. Igarashi, "Drag reduction of a square prism by flow control using a small rod," *Journal of Wind Engineering and Industrial Aerodynamics*, vol. 6971, pp.141-153, 1997.

[8] M. Farhadi, K. Sedighi, and E. Fattahi, "Effect of a splitter plate on flow over a semi-circular cylinder," Proceeding of the Institution of Mechanical Engineering, Part G, *Journal of Aeroscope Engineering,* vol. 224, pp. 321-330, 2010.

[9] K. Kwon, H. Choi, "Control of laminar vortex shedding behind a circular cylinder using splitter plates," *Phys, Fluids*, vol. 8, pp. 479-486, 1995.

[10] S. Ul. Islam, H. Rahman, W. S. Abbasiand T. Shahina, "Lattice Boltzmann study of wake structure and force statistics for various gap spacings between a square cylinder with a detached flat plate," *Arabian Journal for Science and Engineering*, vol. 40, pp. 2169-2182, 2015.

[11] S. Turki, "Numerical simulation of passive control on vortex shedding behind square cylinder using splitter plate," *Engineering Applications of Computational Fluid Mechanics*, vol. 2, pp. 514-524, 2008.

[12] S. Ul. Islam, H. Rahman, W. S. Abbasi, U. Noreen and A. Khan, "Suppression of fluid force on flow past a square cylinder with a detached flat plate at low Reynolds number for various spacing ratios, *Journal of Mechanical Science and Technology*, vol. 28, pp. 4969-4978, 2014.

[13] M. Md. Alam, M. Moriya, K. Takai, and H. Sakamoto, "Suppression of fluid forces acting on two square prisms in a tandem arrangement by passive control of flow," *Journal of Fluids and Structures*, vol. 16, pp. 1073-1092, 2002.

[14] L. Zhou, M. Cheng, and K.C. Hung, "Suppression of fluid force on a square cylinder by flow control," *Journal of Fluids and Structures*, vol. 21, pp. 151-167.

[15] M. S. M. Ali, C. J. Doolan and V. Wheatley, "Low Reynolds number flow over a square cylinder with a detached flat plate," *International journal of Heat and Fluid Flows*, vol. 36, pp. 133-141, 2012.

[16] S. Malekzadeh and A. Sohankar, "Reduction of fluid forces and heat transfer on a square cylinder in a laminar flow regime using a control plate," *International Journal of Heat and Fluid Flow*, vol. 34, pp. 15-27, 2012.

[17] A. Gupta, "Suppression of vortex shedding in a flow around square cylinder using control plate," pp. 1-13, 2013 (home.iitk.ac.in/~gabhinav/Abhinav_Gupta_paper.pdf).

[18] J. Hwang, K. Yang, S. Sun, "Reduction of flow induced forces on a circular cylinder using a detached splitter plate," *Phys. Fluids,* vol. 15, pp. 2433-2436, 2003.

[19] L. Liu, M. Liu, B. Teng, Z. D. Cui, G. Q. Tang, M. Zhao and L. Cheng, "Numerical investigation of fluid flow past circular cylinder with multiple control rods at low Reynolds number," *Journal of Fluids and Structures*. vol. 48, pp. 235-259, 2014.

[20] G. R. Vamsee., M. L. De Tena and S. Tiwari, "Effect of arrangement of inline splitter plate on flow past square cylinder," *Progress in Computational Fluid Dynamics*. vol. 14, pp. 277-293, 2014.

[21] M. Breuer, J. Bernsdorf, T.Zeifer and F. Durst, " Accurate computations of the laminar flow past a square cylinder based on two different methods: Lattice-Boltzmann and finite-volume," *Journal of Heat and Fluid Flows*, vol. 21. pp. 186-196, 2000.

[22] C. J. Doolan, "Bluff body noise reduction using aerodynamic interference," in *Australian Institute of Physics (AIP), 18th National Congress*, Adelaids, South Australia, 2008.

[23] A. Sohanker, C. Norberg and L. Davidson, "Simulation of three dimensional flow around a square cylinder at moderate Reynolds number," *Physics of fluids*, Vol. 11, no. 2, pp. 288-306, 1999.

[24] A. K. Saha, G. Biswas and K. Muralidha, "Three-dimensional study of flow past a square cylinder at low Reynolds number," International journal of Heat and Fluid Flow, Vol. 24, no.1, pp. 54-66, 2003.
[25] Z. Guo, H. Liu, LI. S. Luo and K. Xu," A comparative study of the LBE and GKS methods for 2D near incompressible laminar flows," *Journal of Computational Physics*, Vol. 227, pp. 4955-4976, 2008.
[26] M. Breuer, J. Bernsdorf, T.Zeifer and F. Durst, " Accurate computations of the laminar flow past a square cylinder based on two different methods: Lattice-Boltzmann and finite-volume," *Journal of Heat and Fluid Flows*, Vol. 21. pp. 186-196, 2000.
[27] Y. Dazh, M. Renwei, L.S. Luo, and S. Wei, "Viscous flow computations with the method of lattice Boltzmann equation", *Progress in Aerospace Sciences*, Vol. 39, pp. 329-367,2003.
[28] S. Ul. Islam, W. S. Abbasi, and C. Y. Zhou, "Transitions in the unsteady wakes and aerodynamic characteristics of the flow past three square cylinders aligned inline", *Aerospace Science and Technology*, Vol. 50, pp. 96-111,2016.
[29] S. Ul. Islam, C. Y. Zhou, A. Shah, and P. Xie, "Numerical simulation of flow past rectangular cylinders with different aspect ratios using the incompressible lattice Boltzmann method", *Journal of Mechanical Science and Technology*, Vol. 26, pp. 1027-1041, 2012.
[30] S. Ul. Islam, H. Rahman, C. Y. Zhou, and S. C. Saha, "Comparison of wake structures and force measurements behind three side-by-side cylinders", *Journal of the Brazilian Society of Mechanical Science and Engineering*, DOI 10.1007/s40430-014-0297x.
[31] S. Ul. Islam, W. S. Abbasi, H. Rahman, and R. Naheed, "Numerical investigation of wake modes for flow past three tandem cylinders using the multi-relaxation-time lattice Boltzmann method for different gap spacings", *Journal of the Brazilian Society of Mechanical Science and Engineering*, DOI 10.1007/s40430-014-0282-4.
[32] S. Ul. Islam, W. S. Abbasi, and A. Khan, "The effect of Reynolds numbers for unequal gap spacings on flow past three square cylinders arranged in-line", *Journal of the Brazilian Society of Mechanical Science and Engineering*, DOI 10.1007/s40430-015-0468-4.
[33] H. Rahman, S. Ul. Islam, C. Y. Zhou, T. Kiyani, and S. C. Saha, "On the effect of Reynolds number for flow past three side-by-side square cylinders for unequal gap spacings", *KSCE Journal of Civil Engineering*, Vol. 19, pp. 233-247, 2015.
[34] W. S. Abbasi, S. Ul. Islam, S. C. Saha, Y. T. Gu, and C. Y. Zhou, "Effect of Reynolds numbers on flow past four square cylinders in an in-line square configuration for different gap spacings", *Journal of Mechanical Science and Technology*, Vol. 28, pp. 539-552, 2014.